Acquisition and Analysis of Terahertz Time Domain Imaging and Sensing

Babatunde Ajilore[1], *Student member,* William Baughman[1], *Student member,* Shawn D. Wilbert[1], *Student member,* JongSu Kim[1,2], Patrick Kung[1], and Seongsin Margaret Kim[1]*, *Member*

[1]Department of Electrical and Computer Engineering
The University of Alabama, Tuscaloosa, AL 35487
[2]Department of Image System Science and Engineering,
Pukyong National University, Pusan, 608-739 Republic of Korea
*E-mail: seongsin@eng.ua.edu

***Abstract*—We present results of an acquisition of Terahertz imaging and its analysis in terms of frequency based on a Time Domain Terahertz Spectroscopy System. THz radiation was generated using a photoconductive antenna based on LT-GaAs and was detected by the electro-optical sampling in a ZnTe crystal. Broadband THz pulses were obtained in the range from 0.1 THz to 4 THz, with a peak intensity at 1 THz. The full transmission spectrum for different materials was measured, and frequency-dependent imaging characteristics were analyzed.**

I. INTRODUCTION

The Terahertz (THz) portion of the electromagnetic spectrum, between 0.1 and 10 THz (or 3000 μm to 30 μm wavelength), represents a current frontier for multidisciplinary fundamental research in physics, materials science, chemistry, biology, and medicine with enormous potential opportunities.[1-6] For a long time, Terahertz was not explored because of the lack of appropriate sources and detectors. However, advances in electronics and optoelectronics devices, and in optics have made this portion of the electromagnetic spectrum more attainable to researchers, and opened new windows of abundant applications in many different fields of research.

Practical applications have been feasible in the areas of spectroscopy, sensing and imaging such as: medical imaging [7,8], industrial imaging for package inspection and non destructive testing [9], gas sensing [10], gas phase spectroscopy, time-resolved studies, THz ranging and sensing, biological spectroscopy including bio-warfare agent detection [11], explosive detection [12], and astronomy [2]. Some of these applications stem from the unique ability of THz wavelengths to safely penetrate a wide variety of non-conducting materials including clothing, paper, cardboard, wood, masonry, plastic and ceramics. THz radiation is the most suitable way to inspect any device and contents in a sealed container.

Terahertz Time Domain Spectroscopy (TDS) has been one of the most successful techniques to generate and detect THz radiation without cryogenic cooling, and it carries both the amplitude and phase information of the traveling THz radiation. As a result of the direct time resolved detection of the THz pulse electric field, unique information about the scattering mechanisms can be extracted from the TDS data in addition to being able to yield imaging contrast in the THz. There is still limited performance in imaging due to the difficulties of constructing the large arrays of pixels using TDS compared other multipixel detectors. However, only TDS can convey the full spectroscopic information for each pixel.

II. EXPERIMENTAL SET-UP

The experimental set-up is shown in Fig. 1. It consists of a Terahertz TDS system manufactured by Zomega, Inc, and pumped by a mode-locked Ti:Sapphire ultrafast laser emitting 120 fs pulses at a wavelength of 780 nm, a repetition rate of 76 MHz and an average power of 120 mW. The pulses are split into a pump beam and a probe beam. The pump beam is focused onto a low-temperature grown GaAs (LT-GaAs) photoconductive antenna integrated with a Silicon lens while a high voltage bias is pulsed across the antenna. The transient photocurrent was obtained from the relaxation of free carriers photogenerated by the femtosecond pulses.

The probe beam is guided via a delay line to detect the THz radiation through the electro-optics sampling. In this method of detection, the Terahertz beam induces birefringence in the ZnTe electro-optic crystal; as the probe beam is passed collinearly into the crystal it

This work is funded by the National Science Foundation under grant no. ECCS#0824452. J.S.K. thanks the support of LG Yonam Foundation Faculty Fellowship.

becomes elliptically polarized proportionally to the intensity of the terahertz radiation. The horizontal and vertical components of the beam are split and sent to two separate photodiodes for balanced detection. The resulting voltage difference is synchronously measured using a lock-in amplifier to directly yield the received terahertz electric field intensity.

By moving the variable position delay stage, the complete Terahertz waveform can be obtained. The movement of the delay stage leads to a path length difference between the terahertz beam and probe beam, corresponding to a time delay in beam propagation in the picosecond scale. In the transmission measurement configuration, polyethylene lenses are used to focus the terahertz on the sample with a spot size of 0.5 mm.

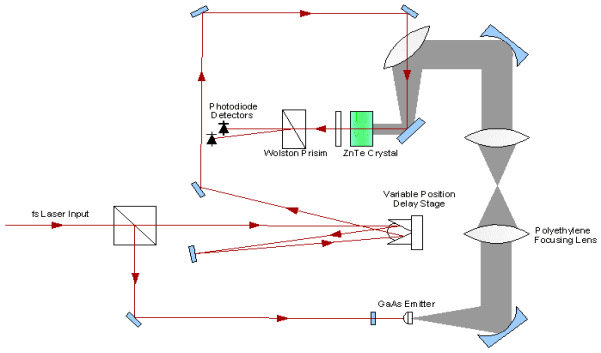

Figure 1. Schematic set-up of the THz imaging system.

Typical THz signals measured after passing through different materials are shown in Fig. 2. The pulse width is about 0.5 ps and we observed ringing of the pulse mainly due to moisture in the laboratory. Purging with dry nitrogen can improve the pulse shape and minimize the ringing. The time domain THz pulse is then converted into the frequency domain using fast Fourier transform (FFT). We are able to obtain broadband THz pulses in the range from 0.3 THz to 4 THz, with the peak intensity at 1 THz.

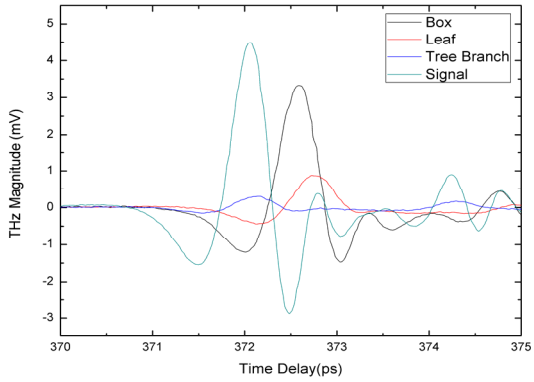

Figure 2. Measured time domain electric field amplitudes of the Terahertz signal transmitted through different materials.

It is important to note three parameters of the system performance: peak magnitude, waveform shape, and signal-to-noise ratio (SNR). The peak magnitude and waveform shape of the generated terahertz output are directly affected by the optical alignment, pump beam incidence angle to the photoconductive antenna, and alignment of ZnTe crystals. An increased SNR can also be observed after using an additional reflective lining to reduce interference and scattering. The maximum SNR of our system could reach up to 100 dB at its best performance.

III. Results and Discussion

A. *Transmission Measurements*

Transmission measurements are often used to determine the specific absorption features of certain materials and to obtain specific fingerprints at resonant absorption frequencies of the constituent molecules. Terahertz transmission characteristics can be analyzed in both the time and frequency domains.

The time domain signal of the THz radiation propagating in free space is shown in Fig. 2 as a function of the time delay between the pump and probe beams. By comparing the magnitude change and delay time shift resulting from the transmission through a sample with the reference signal of Fig. 2, the Terahertz absorption properties of the probed material can be determined.

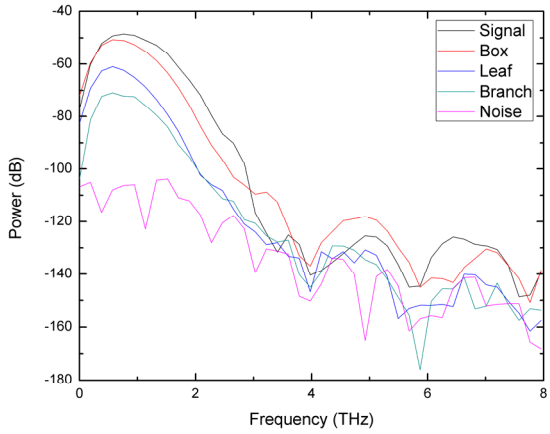

Figure 3. Measured transmitted THz power frequency spectrum after passing through free space ('signal') and the same materials as shown in Fig. 2. The noise floor is shown as well.

More precise analysis can be done in the frequency domain. For example, the absorption spectrum, complex refractive index, complex conductivity characteristics of the material in question can be derived from the changes in transmission as a function of THz frequency. Fig. 3 shows the power spectrum as a function of frequency for the transmitted Terahertz signal through free space and through the same materials as shown in Fig. 2, along with the system noise floor.

B. *Acquisition of THz Imaging*

Imaging in the Terahertz can be accomplished by scanning the THz beam across a sample and collecting transmission data.

In the system we designed, data are acquired one pixel at a time. The sample to be imaged is placed at the focal plane of the focusing lenses in the THz beam path and attached to a motion microcontroller that features three translational degrees of freedom. The x-axis and z-axis move the sample within the plane perpendicular to the THz radiation. If focusing mirrors are used, the y-axis motion of the microcontroller allows precise positioning of the sample in the focal plane and thus adjustment of the sharpness of the resulting image. Using the motion controller, the sample is translated about the THz beam focal point and the transmission data for each point in the predefined spatial matrix of points that constitutes the imaging range are collected.

Control of the image acquisition is achieved through an in-house software written using LabVIEW. Data analysis and image reconstruction is written using Matlab. Two acquisition modes have been investigated: normal-acquisition mode and fast-acquisition mode.

In normal-acquisition mode, the entire THz time domain and frequency domain spectra are collected for each pixel sequentially by changing the time delay between the pump and the probe beams, along with the sample physical position in space. This results in a large data set for each pixel that can be further filtered through several methods as described in the following section C.

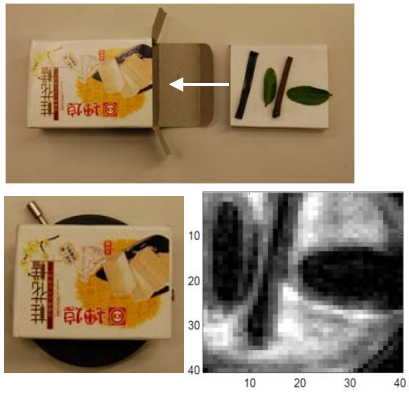

Figure 4. (top) Photograph of a piece of wood, and leaves (bottom left) enclosed in carboard box. (bottom right) Terahertz image of concealed objects in enclosed box acquired in fast-acquisition mode.

By contrast, in fast-acquisition mode, the time delay between the pump and the probe beams is fixed to a value that results in a strong THz electric field amplitude being detected when unobstructed. The change in amplitude of the THz radiation electric field at that fixed value of time delay is then the only data collected for each pixel. This dramatically cuts the time required to acquire an image by a factor of up to 5~6, but it comes at the expense of reduced information about the sample.

Fig. 4 shows an example of Terahertz transmission image obtained using the fast-acquisition mode from a few pieces of wood and fresh tree leaves concealed in a cardboard box. The image is composed of 40×40 pixels with a pixel pitch of 0.5 mm. This illustrates the ability of THz wavelengths to penetrate cardboard materials while being blocked by water containing compounds.

C. *Normal-Acquisition Mode Imaging Analysis*

A straightforward technique to filter and analyze the data collected in the normal-acquisition mode is to extract the amplitude of the THz electric field at any specific position in the space/time domain for each pixel. A slight variation on this technique would be to use the peak-to-peak value of the signal instead. As such, the data obtained in fast-acquisition mode represents a sub-set of the data that could be obtained in normal-acquisition mode. This is illustrated in scans made on the sample shown in the photograph in Fig. 5. It consists of a letter 'F' formed using zinc powder stuck on adhesive tape on two strips of tape that slightly overlap at the center along the vertical direction, as shown in the photograph.

Figure 5. Photograph of the letter 'F' formed with zinc powder. The powder was held with adhesive tape.

Fig. 6 shows a series of images of the letter "F" obtained using our TDS system after data cube filtering using several algorithms that we developed. Fig. 6(a) shows the THz image constructed by extracting the maximum amplitude in the THz time domain at each pixel. This maximum can occur at different values of time delay between the pump and the probe beams for different pixels. Fig. 6(b) is obtained by taking into extracting the THz signal amplitude in the time domain at an arbitrarily chosen value of time delay.

More advanced frequency domain analysis is also possible by extracting the THz transmitted signal power at the same specific frequencies for all pixels. This is illustrated in Fig. 6(c) through (e), which shows that a clear contrast difference can be achieved by analyzing the data at different frequencies. At 0.37 THz, there is almost

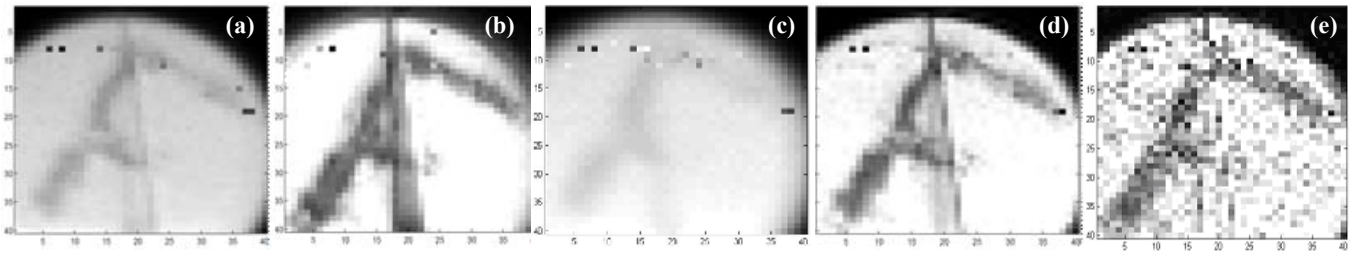

Figure 6. Terahertz images of the letter 'F' formed with zinc powder on adhesive tape using: (a) maximum amplitude in the time domain, (b) amplitude in the time domain at a fixed value of time delay; (c) – (e) power at a fixed frequency of 0.1 THz, 1.7 THz and 2.45 THz, respectively.

no contrast between the zinc powder, the adhesive tape and the tape overlap region. At 1.7 THz, a much better contrast is obtained between the zinc powder and the tape, as well as between the tape and the adhesive overlap region, but there is little contrast between the zinc powder and the adhesive overlap region. At 2.45 THz, there is still a good contrast between the zinc powder and the tape, but the overlap region becomes faded out. This shows that significant amount of information can be extracted through THz imaging.

The clear differences in contrast can be attributed to the different absorption coefficients of each contributing elements (tape, double tape, and Zn powder) in terms of the frequency in the range between 0.1 THz and 5 THz.

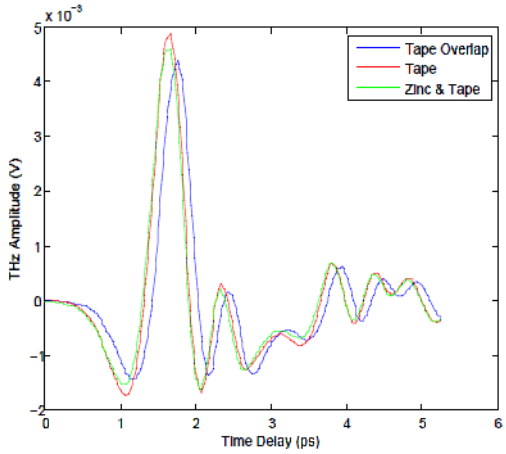

Figure 7. Measured time domain THz electric field amplitudes for tape, tape overlap, and zinc powder stuck on adhesive tape.

Fig. 7 illustrates some of these differences in the THz transmission signal in time domain spectrum as a function of the material through which the THz radiation is transmitted. The transmission curves associated with the regions with zinc powder and those without are similar in shape. However, the signal through the zinc powder stuck on tape is slightly diminished from that through the tape itself. In addition, in the overlapped tape region, the THz signal is slightly delayed in time, potentially due to the extra thickness of this region. This delay could in turn be used to determine the thickness of this layer.

IV. Conclusion

In summary, we have presented THz imaging and sensing results using THz Time Domain Spectroscopy in the transmission mode. A number of imaging modes and analysis methods have been demonstrated. Time domain and frequency domain imaging were carried out and compared.

References

[1] DOE-NSF-NIH Workshop on "Opportunities in THz Science", Arlington, VA, February 12-14, 2004.

[2] P.H. Siegel, "Terahertz technology," *IEEE Transactions on Microwave Theory and Techniques* 50, 910 (2002).

[3] P.H. Siegel, "Terahertz technology in biology and medicine," *IEEE Transactions on Microwave Theory and Techniques* 52, 2438 (2004).

[4] X.C. Zhang, "Terahertz technology and applications," *SPIE Photonics West short course*, San Jose, CA, 2005.

[5] M. Shur, "Terahertz technology: devices and applications," *Proceedings of ESSDERC* 2005.

[6] D.M. Mittleman, M. Gupta, R. Neelamani, R.G. Baraniuk, J.V. Rudd, and M. Koch, "Recent advances in terahertz imaging," *Applied Physics B 68*, 1085 (1999).

[7] D. Armone, C. Ciesla, and M. Pepper, "Terahertz imaging comes into view," Physics World 13, 35-40 (2000).

[8] K. Humphreys, J.P. Loughran, M. Gradziel, W. Lanigan, T. Ward, J.A. Murphy, Oapos, and C. Sullivan, "Medical applications of terahertz imaging: a review of current technology and potential applications in biomedical engineering," *Engineering in Medicine and Biology Society*, 2004, IEMBS' 04, 26th Annual International Conference of the IEEE, vol. 1, 1302 (2004).

[9] W.L. Chan, J. Deibel, and D.M. Mittleman, "Imaging with terahertz radiation," *Reports on Progress in Physics* 70, 1325 (2007).

[10] D.M. Mittleman, R.H. Jacobsen, R. Neelaman, R.G. Baraniuk, and M.C. Nuss, "Gas sensing using terahertz time-domain spectroscopy," *Applied Physics B* 67, 379 (1998).

[11] D.L. Woolard, E.R. Brown, A.C. Samuels, J.O. Jensen, T. Globus, B. Gelmont, and M. Wolski, "Terahertz-frequency remote-sensing of biological warfare agents," *Microwave Symposium Digest*, 2003 IEEE MTT-S International, vol. 2, 763 (2003).

[12] J.S. Melinger, N. Laman, and D. Grischkowsky, "The underlying terahertz [vibrational spectrum of explosive solids," *Applied Physics Letters* 93, 011102 (2008).